Acta Pharmacologica Sinica 2005 Aug; 26 (8):1000 –1008

Full-length article

Cytotoxicity, apoptosis induction, and mitotic arrest by a novel podophyllotoxin glucoside, 4DPG, in tumor cells[1]

Yi-lin QI[2,4], Fan LIAO[2,4], Chang-qi ZHAO[2], Yong-da LIN[2], Ming-xue ZUO[2,3,5]

[2]College of Life Sciences, Beijing Normal University, Beijing 100875, China; [3]Key Laboratory for Molecular Biology and Gene Engineering Drugs of Beijing, Beijing 100875, China

Key words

4-demethyl-picropodophyllotoxin 7'-*O*-β-*D*-glucopyranoside; podophyllotoxin; flow cytometry; microtubulin; apoptosis

[1] Project supported by the National Natural Science Foundation of China (No 30270449; No 30370196) and Beijing Natural Science Foundation (No 5052016).
[4] The two authors contributed equally to this work
[5] Correspondence to Prof Ming-xue ZUO.
Phn 86-10-5880-8558
E-mail mxzuo@bnu.edu.cn

Received 2005-04-01
Accepted 2005-04-11

doi: 10.1111/j.1745-7254.2005.00148.x

Abstract

Aim: To define the *in vitro* cytotoxic activities of 4-demethyl-picropodophyllotoxin 7'-*O*-β-*D*-glucopyranoside (4DPG), a new podophyllotoxin glucoside. **Methods:** Antiproliferation activity was measured in several tumor cell lines by using the microculture tetrazolium MTT assays. Cell cycle distribution was analyzed using flow cytometry and mitosis index assays. Furthermore, transmission electron microscopy, TUNEL, DNA agarose electrophoresis, and activated caspase-3 were used to analyze the induction of apoptotic cell death. Moreover, intracellular changes in the cytoskeleton were detected using immunocytochemistry. **Results:** 4DPG effectively inhibited the proliferation of cancer cells (HeLa, CNE, SH-SY5Y, and K562 cell lines). For the K562 cell line, the antiproliferation effect of 4DPG was much more potent than that of etoposide (IC_{50} value: 7.79×10^{-9} mol/L for 4DPG *vs* 2.23×10^{-5} mol/L for etoposide). Further, 4DPG blocked the cell cycle in the mitotic phase. The induction of apoptosis and elevated levels of activated caspase-3 were confirmed in cells treated with 4DPG. The microtubule skeleton of HeLa cells was disrupted immediately after treatment with 4DPG. **Conclusion:** The cytotoxicity of 4DPG is due to its inhibition of the microtubule assembly of cancer cells at a low concentration, thus inducing apoptosis. These properties qualify 4DPG to be a potential antitumor drug.

Introduction

Natural products have long been an important source of treatments for cancer. At present, there are more than one thousand plants that have been found to possess significant anticancer properties. Although many molecules obtained from plants have been shown to have antineoplastic activity, a huge number of molecules still remain to be isolated or studied in detail. Recently, traditional Chinese medicines have attracted much interest, and evaluations of potential antineoplastic herbal ingredients are currently being carried out in laboratories[1–3].

Of the natural compounds with anticancer properties, podophyllotoxin occupies a very important position[4]. Podophyllotoxin is a naturally occurring lignan, which is isolated from the dried roots and rhizomes of *Podophyllum* plants, and has been proven to possess antineoplastic properties. Although its unacceptable levels of cytotoxicity precluded the use of podophyllotoxin as an anticancer drug, subsequent research aimed to abstract and synthesize new analogues of podophyllotoxin, and analyzed podophyllotoxin's structure-function relationship and its mechanism of action. Several decades' efforts have proven that the cytotoxicity of podophyllotoxin is due to its interaction with β-tubulin, because it disrupts microtubule organization and leads to mitotic arrest, in a manner that is similar to the action of colchicines[5–8]. Meanwhile, many analogues of podophyllotoxin have been determined, and most exhibit pronounced biological activity as strong antiviral or antineoplastic agents[4,9–11]. Among these molecules, etoposide is a notably successful derivative of podophyllotoxin[12,13], with demonstrated efficacy against a broad spectrum of human

malignancies, including testicular, germ cell, lung, and other cancers[14–17]. Etoposide arrests cancer cell growth prior to mitosis as a DNA topoisomerase II inhibitor[18–21], whereas podophyllotoxin has no inhibitory effect on this enzyme[22]. Conversely, an isomer of podophyllotoxin, picropodophyllotoxin, has no inhibitory effect on microtubules and apparently lacks cytotoxicity[4,22–26]. After these observations were made, little or no attention was paid to picropodophyllotoxin. However, some recent studies on picropodophyllotoxin produced different and exciting results. Some derivatives of picropodophyllotoxin have high levels of antiproliferation activity against the L1210 cell line because they inhibit microtubule assembly[27]. The cyclolignan podophyllotoxin and picropodophyllotoxin inhibit tyrosine phosphorylation of the insulin-like growth factor-1 receptor (IGF-1R), but have no effect on the highly homologous insulin receptor (IR) or tyrosine kinases that are related to other major cancer-relevant growth factor receptors, so they specifically inhibit malignant cells[28,29]. These results could cause more research interest to be focused on the analogues of podophyllotoxin, in order to identify the derivatives with the most potent and specific antitumor activity (ie, to optimize the structure), or to develop an alternative and renewable source of podophyllotoxin.

Sinopodophyllum emodi (Wall) Ying, mainly distributed over the Western region of the Qinling mountains of China, is a type of *Podophyllum*. In the area in which it is grows, *S emodi* has been used as a folk medicine to treat cancer and various types of verrucosis, but the pharmacology of its constituent ingredients has not been investigated. Our previous study revealed that 4-demethyl-picropodophyllotoxin 7'-*O*-β-*D*-glucopyranoside (4DPG) (Figure 1) is a novel podophyllotoxin glucoside isolated from *S emodi*[30]. A significant structural characteristic of 4DPG is that it belongs to the picropodophyllin family. Therefore, as a herbal medicine ingredient and a podophyllotoxin analogue with a quite different structure, we wondered what the biological activity of this molecule would be.

In this study, we demonstrate that 4DPG is a highly potent inhibitor of microtubule assembly, leading to mitotic arrest, induction of apoptosis, and inhibition of the proliferation of malignant cells.

Materials and methods

Chemicals 4DPG was isolated from *Sinopodophillum emodi* (Wall) Ying (Berberidaceae) by our group[30]. The extracted 4DPG was dissolved in methanol (0.01 mol/L) and stored at room temperature.

Cell lines and cell culture A human cervical carcinoma cell line (HeLa), a human nasopharyngeal carcinoma cell line (CNE) and a human neuroblastoma cell line (SH-SY5Y) were grown in Dulbecco's MEM (Hyclone, Logan, USA) and a human chronic myelogenous leukemia cell line (K562) was maintained in RPMI-1640, supplemented with 10% heat-inactivated fetal calf serum (FCS), 100 U/mL penicillin and 100 μg/mL streptomycin in a humidified atmosphere (37 ºC, 5% CO_2).

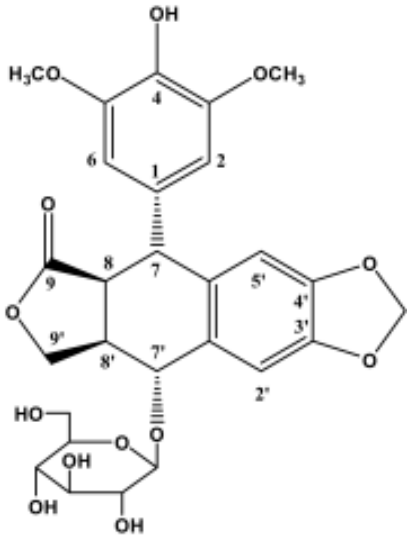

Figure 1. Chemical structure of 4DPG.

Cytotoxicity assay The MTT assay to determine the cytotoxicity of 4DPG was performed as described previously[31]. Briefly, cells were plated onto 96-well plates at 2×10^3 cells per well for the HeLa, CNE, and SH-SY5Y cell lines or at 5×10^3 cells/well for the K562 cell line. After incubation with medium containing 0.1% methanol, 2×10^{-5} mol/L 4DPG and etoposide (VP-16) for 48 h, MTT (Sigma Chemical Co, St Louis, USA) was added to cell cultures to a final concentration of 0.5 mg/mL and incubated at 37 ºC for 4 h. Then, the adherent cells were solubilized with 200 mL dimethyl sulfoxide (Me_2SO, Sigma), and K562 cells were exposed to 100 mL 0.04 N 2-propanolic hydrochloric acid. Absorbance at 570 nm was measured on a multiplate reader (Bio-Rad 550, Hercules, USA).

In the same way, K562 cells treated with gradient concentrations of 4DPG and etoposide for 48 h were tested. The drug concentration required to inhibit cell growth by 50% (IC_{50}) was determined by interpolation from dose-response curves. All assays were carried out in quadruplicate. The inhibition rate of cell proliferation was calculated by:

$$\text{Inhibition rate (\%)} = \frac{OD_{\text{control}} - OD_{\text{treated}}}{OD_{\text{control}}} \times 100\%$$

Cell cycle analysis K562 cells were treated with 1×10^{-9} mol/L, 1×10^{-8} mol/L,1×10^{-7} mol/L, and 1×10^{-6} mol/L 4DPG, respectively. After incubation for 48 h, cells were collected and fixed with 70% ethanol at 4 ºC for 24 h, then stained with 50 μg/mL propidium iodide (Sigma). The cell cycle distribution from 10 000 cells was collected by using the Epics flow cytometer (Coulter Electronics, Fullerton, USA). Cell cycle analysis was performed by using Multicycle software (Phoenix Flow Systems, San Diego, USA).

The mitotic index was determined by Giemsa staining. K562 cells were incubated with or without 1×10^{-6} mol/L 4DPG for 48 h. Then, fixed cells were stained with Giemsa solution and mitotic cells were counted per visual field. Quadruplicate fields were measured.

DNA fragmentation assay K562 cells were exposed to 0.01% methanol, 1×10^{-6} mol/L 4DPG and 1×10^{-6} mol/L etoposide for 48 h, and then cells were collected by centrifugation. Total DNA was purified with a DNA isolation kit (R&D Systems, Minneapolis, USA) according to the manufacturer's protocol. The DNA was separated in 1.5% agarose gel and visualized by ultraviolet illumination after staining with ethidium bromide.

TUNEL assay After incubation with 1×10^{-6} mol/L 4DPG for 12 h, 24 h, and 48 h, cells were rinsed three times with phosphate-buffered saline (PBS) and fixed with methanol. Based on the TUNEL protocol (Roche, Basel, Switzerland), cells were permeabilized with 0.1% Triton X-100 in 0.1% sodium citrate and then rinsed twice with PBS. The DNA nick-labeling reaction was performed using 50 μL TUNEL reaction mixture, including 45 μL enzyme solution and 5 μL nucleotide mix at 37 ºC for 60 min. Then the samples were rinsed three times with PBS and analyzed under a fluorescence microscope.

Morphology analysis by transmission electron microscopy K562 cells treated with 1×10^{-6} mol/L 4DPG were washed with PBS, centrifuged, and pre-fixed with 2.5% glutaraldehyde in 0.1 mol/L phosphate buffer at 4 ºC for 2 h. The cells were then rinsed thoroughly in phosphate buffer and post-fixed in 1% OsO_4 at 4 ºC for 30 min. After being fixed, the cells were pelleted in 2% agar, then cell blocks were prepared, dehydrated through a graded ethanol series, and embedded in Epon 812 (Spi supplies, West chester, USA). The ultrastructure of cells was analyzed in ultrathin sections in a transmission electron microscope (Hitachi H-600, Tokyo, Japan) after the sections were stained with uranyl acetate and lead citrate.

Caspase-3 cleavage assay After the K562 cells were treated with 10^{-6} mol/L 4DPG as described above, the cells were fixed and incubated with cleaved caspase-3 (Asp175) antibody (Cell Signaling, Beverly, USA) as a primary antibody, which specifically recognizes activated caspase-3 resulting from cleavage adjacent to Asp175, and then with biotinylated goat antirabbit IgG as a secondary antibody. Finally, the cells were incubated with the ABC kit (Vector, Peterborough, England) and visualized by incubation with the colorigenic substrates (DAB, Promega, Madison, USA).

Indirect immunofluorescence staining Exponentially growing HeLa cells were seeded into 96-well plates, then after 12 h, the medium was replaced with complete medium containing 10^{-6} mol/L 4DPG. After treatment with 4DPG for 1 h, 2 h, 3 h, 12 h, 24 h, or 48 h, immunofluorescence staining was performed. The cells were incubated with anti-α-tubulin antibody (ZSBiO, Beijing, China) as a primary antibody, which was followed by a secondary antibody, TRITC-conjugated rabbit antimouse IgG. After being washed three times with PBS, the labeled cells were observed and photographed with a fluorescence microscope (Olympus IX70, Tokyo, Japan).

HeLa cells plated onto cover slips were treated with the 10^{-6} mol/L 4DPG for 24 h. As per the procedure described earlier, the cytoskeletons of the adherent and suspension cells were photographed on a confocal laser scanning biological microscope (Olympus Fluoview FV300).

Statistics Data were expressed as mean±SD and analyzed using two-way analysis of variance (ANOVA). The differences between two groups were determined by using the *t*-test, and statistical significance was set at $P<0.05$.

Results

Chemical structure of 4DPG 4DPG, as a congener of podophyllotoxin, has the same multiple ring structure; however, it differs with respect to the composition and minor modifications of the podophyllotoxin rings, including the steric orientation of a carbon-carbon bond and substitution on the ring. 4DPG has a hydroxy group in the 4-carbon position, but podophyllotoxin has a methoxy group at this position. Another site that differs is the 7'-carbon position, which is substituted in podophyllotoxin with an unmodified glucoside. Among the analogues of podophyllotoxin reported previously, 4DPG is the isomer of the 4'-demethylpodophyllotoxin glucoside DMPG[22].

Effect of 4DPG on proliferation of tumor cells As shown in Figure 2, 4DPG induced a significant inhibition of proliferation in the tested cell lines (SH-SY5Y, CNE, HeLa and K562). Compared with etoposide, 4DPG had much more potent cytotoxic effect on CNE and K562 cells.

After a 48 h-treatment, 4DPG had maximal cytotoxic effect on K562 cells at a concentration of 1×10^{-8} mol/L. The

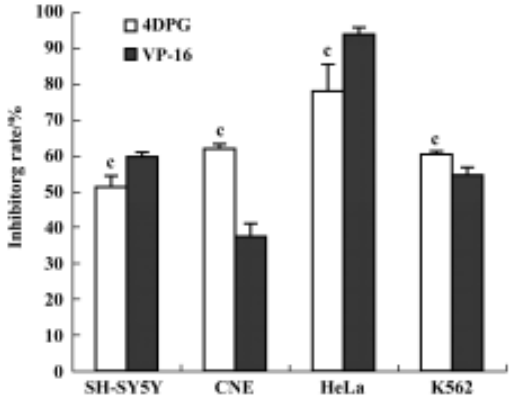

Figure 2. The inhibitory effect of 4DPG on the proliferation of four tumor cell lines (SH-SY5Y, CNE, HeLa, K562) was measured by MTT assays after treatment with 4DPG for 48 h. n=4. Mean±SD. ^cP<0.01 *vs* VP-16.

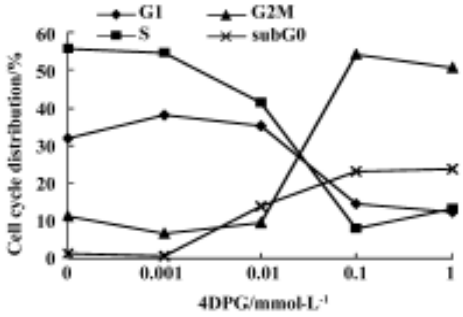

Figure 4. The effect of 4DPG on G2/M phase arrest and induction of apoptosis in K562 cells was dose-dependent. K562 cells were treated with 1×10^{-9} mol/L, 1×10^{-8} mol/L, 1×10^{-7} mol/L or 1×10^{-6} mol/L 4DPG for 48 h. The negative control was the vehicle-treated sample.

maximal inhibition rate was 72.82%, and the IC_{50} value was 7.79×10^{-9} mol/L (Figure 3). Under the same conditions, the maximal effect on cell proliferation inhibition was observed with etoposide at a concentration of 2.5×10^{-4} mol/L , which inhibited 95.25% of cells, with an IC_{50} value of 2.23×10^{-5} mol/L (data not shown).

Mitotic arrest was induced by 4DPG treatment As shown in Figure 4, 4DPG caused a significant dose-dependent accumulation of K562 cells in the G2/M and sub-G0 phases, and a decrease in the G0/G1 and S phases from 1×10^{-9} mol/L to 1×10^{-6} mol/L at 48 h. The differences in cell cycle distribution between vehicle-treated K562 cells and 1×10^{-8} mol/L, 1×10^{-7} mol/L, 1×10^{-6} mol/L treatment are statistically significant (P<0.01).

To further characterize the cell cycle distribution, mitotic index detection was performed. We found that approximately 50% of cells treated with 10^{-6} mol/L 4DPG for 48 h were blocked in mitosis, which was consistent with the result from flow cytometry, but for vehicle-treated cells, only 6.8% were in mitosis (P<0.01).

4DPG induced apoptosis in K562 cells 4DPG treatment resulted in the formation of a DNA ladder in K562 cells at 48 h (Figure 5), but etoposide did not produce the same result. Additionally, as shown in Figure 6, the longer K562 cells were exposed to 1×10^{-6} mol/L 4DPG, the more cells that had DNA strand breaks were labeled by TUNEL.

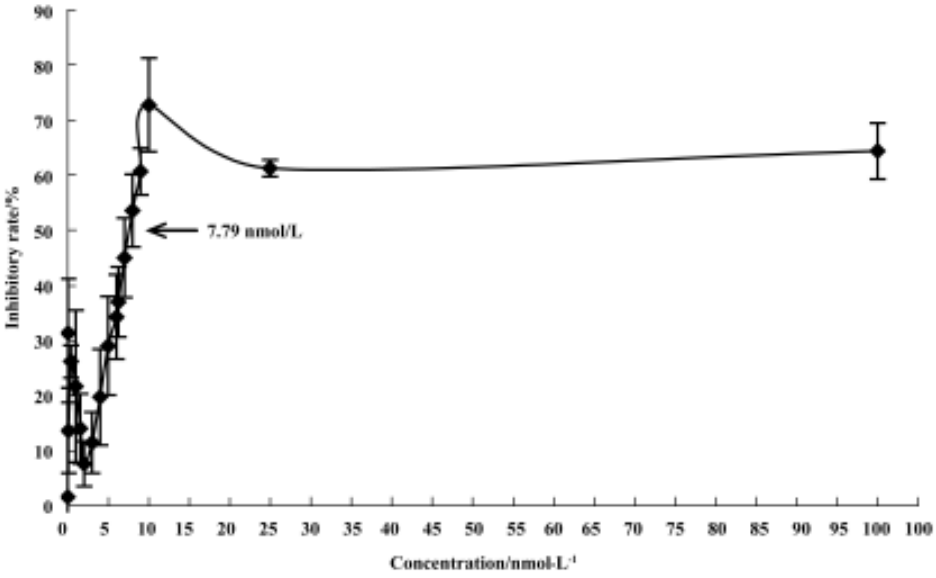

Figure 3. Dose-response curve for the inhibition of cell proliferation. K562 cells were incubated with gradient concentrations of 4DPG for 48 h. n=4. Mean±SD. The inhibition value was calculated using the means of $OD_{control}$ and $OD_{treated}$.

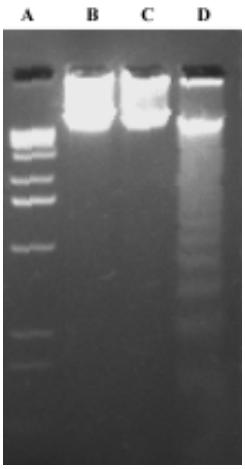

Figure 5. DNA fragmentation in K562 cells treated with 4DPG for 48 h. Lane A: 1 kb marker; lane B: normal control; lane C: treated with 1×10^{-6} mol/L etoposide for 48 h; lane D: treated with 1×10^{-6} mol/L 4DPG for 48 h.

Observations of ultrastructure showed that K562 cells displayed the characteristics of apoptosis after the incubation of 1×10^{-6} mol/L 4DPG for 24 h and 48 h, respectively. That is, some slim protuberances packed with the unit membrane and numerous substances were released around the cell; this was followed by increases of the structure of the membrane in the cytoplasm, and the cytoplasm was separated into several units in which a few vacuoles could be seen; then, the nuclear membrane became unclear, and the chromatin condensed and turned into single chromosome spots (Figure 7).

4DPG induced the activation of caspase-3 As shown in Figure 8, after incubation with 1×10^{-6} mol/L 4DPG for 12 h, the number of activated caspase-3-positive cells had changed little; however, the number had increased greatly after 24 h, and further increased after 48 h.

4DPG inhibited microtubule polymerization At 1 h after 1×10^{-6} mol/L 4DPG treatment, a marked inhibition of microtubule assembly in HeLa cells was observed. Compared with the vehicle-treated cells, the most significant change was the disappearance of the bipolar mitotic spindles in the cell division phase (Figure 9). Additionally, the results from confocal fluorescent microscopy further confirmed that 4DPG

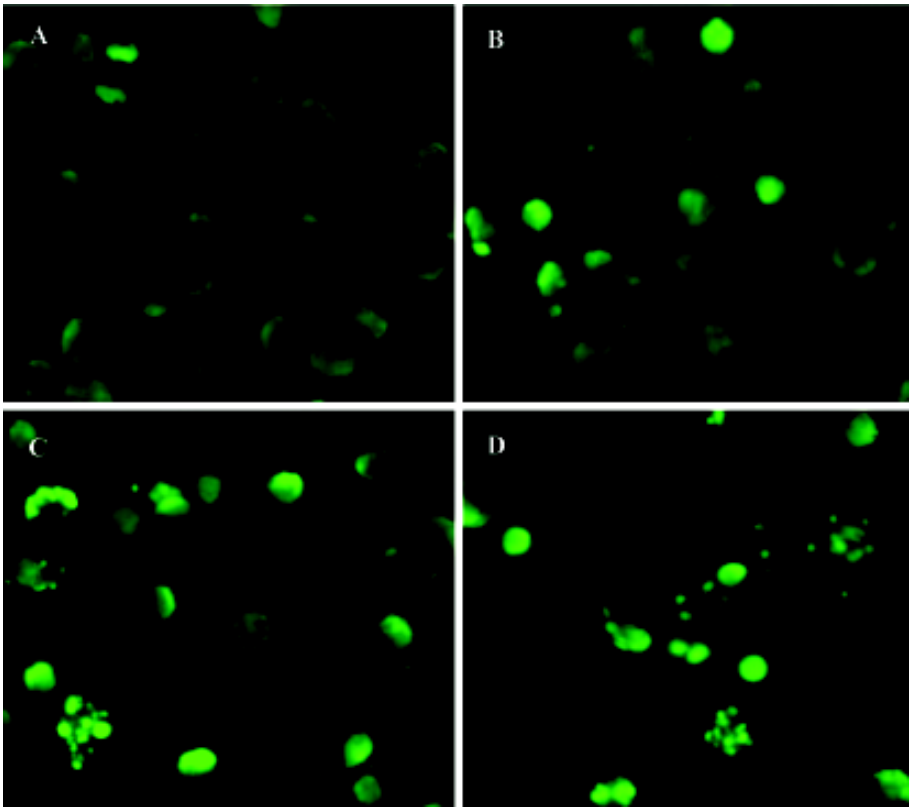

Figure 6. DNA breaks induced by 1×10^{-6} mol/L 4DPG were detected by TUNEL. (A) Vehicle-treated K562 cells (only cells involved in mitosis were positively labeled); (B) after 12 h exposure, the chromatin in a few cells condensed and broke; (C) after 24 h exposure, many more cells were positively labeled; (D) after 48 h exposure, condensed and separated chromatins were dispersed in the cytoplasm (×400).

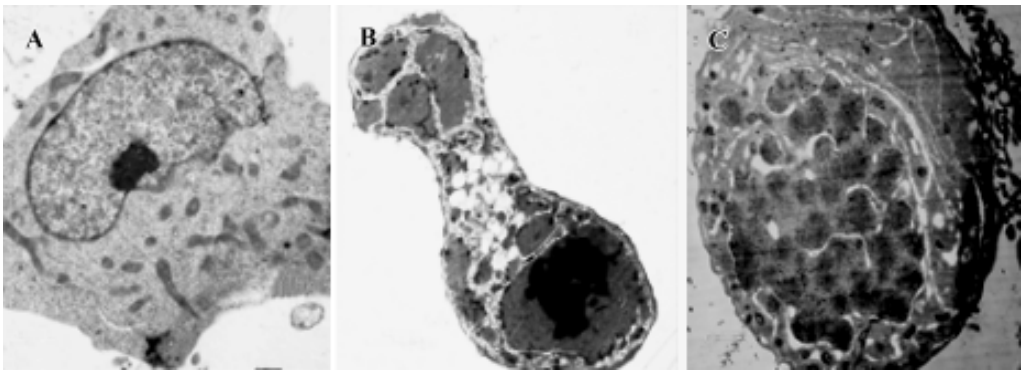

Figure 7. Ultrastructural photomicrographs of K652 cells after treatment with 1×10^{-6} mol/L 4DPG, visualized by transmission electron microscopy. (A) Normal control, the nucleolus and nuclear membrane were clear, chromatin was dispersed and uncondensed (×5000); (B) after 4DPG treatment for 24 h, the nucleolus disappeared and the nuclear chromatin was condensed (×3500); (C) after treatment with 4DPG for 48 h, the nuclear membrane was becoming unclear, and the chromatin was condensed and separated. Cells displayed the characteristics of apoptosis and mitosis (×5 000).

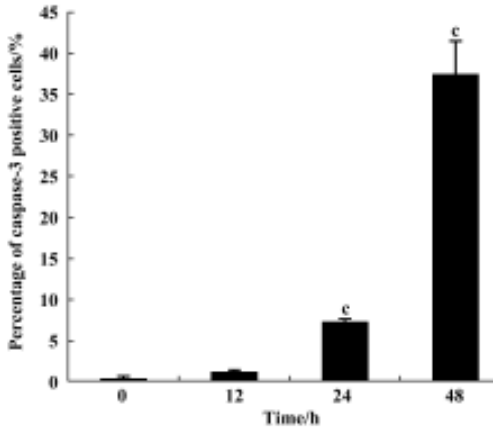

Figure 8. The percentage of activated caspase-3 in K562 cells increased greatly with increased exposure to 1×10^{-6} mol/L 4DPG. n=4. Mean±SD. ^cP<0.01 *vs* 0 h.

disrupted normal microtubule polymerization (Figure 10).

Discussion

By screening new potential antitumor agents using a cytotoxicity assay, we identified 4DPG as an agent that possessed antiproliferative properties. 4DPG has been found to have an extensive and significant inhibitory effect on the proliferation of various carcinoma cell lines. In this study, we found that compared with etoposide, 4DPG is much more potent in some cell lines, such as HeLa and K562. The IC_{50} value of 4DPG on K562 cells was 2–3 orders of magnitude lower than that of etoposide. The cytotoxic effect of 4DPG on K562 cells is dose-dependent. Furthermore, regarding the effect of 4DPG on the cell cycle distribution, 4DPG was found to cause significant mitotic arrest in K562 cells. These findings regarding the picro derivatives are different from those reported previously, which considered that these compounds lacked biological activity and that the C-8α, C-8'βtrans configuration is of crucial importance for biological activity[4]. However, recent studies on a new derivative of picropodophyllotoxin, 4-amino-4 deoxypicropodophyllotoxin, have proven that it exerts antitumor activity through inhibiting microtubule assembly[27]. These results suggest that the modification of picropodophyllotoxin with a free hydroxy group in the 4-position or substitution at the 7'-position can also produce molecules with high levels of biological activity. Moreover, the specific inhibitive effect of tyrosine phosphorylation of IGF-1R and malignant cell growth by picropodophyllotoxin that was observed by Girnita and coworkers provide another perspective on this molecule[28,29]. These new discoveries suggest that picro derivatives retain a high biological activity and could become an important family of anticancer agents.

In the podophyllotoxin family, there are two well-investigated mechanisms that cause cytotoxicity[4]. The first is the inhibition of microtubule polymerization (eg, podophyllotoxin[5,6]) and the second is the inhibition of topoisomerase II (eg, etoposide[18]). As shown in Figure 8, after just 1 h exposure to 4DPG, the fibroid microtubule skeleton in normal HeLa cells was broken and the tubulin-α tagged by TRITC was distributed in the cytoplasm homogeneously. These observations indicate that the cytotoxicity of 4DPG is caused by disrupting the microtubule assembly, which interferes with mitosis at low concentrations. This property is similar to that of podophyllotoxin, indicating that 4DPG is a new antimicrotubule agent. However, reports regarding the effectiveness of podophyllotoxin and picropodophyllotoxin

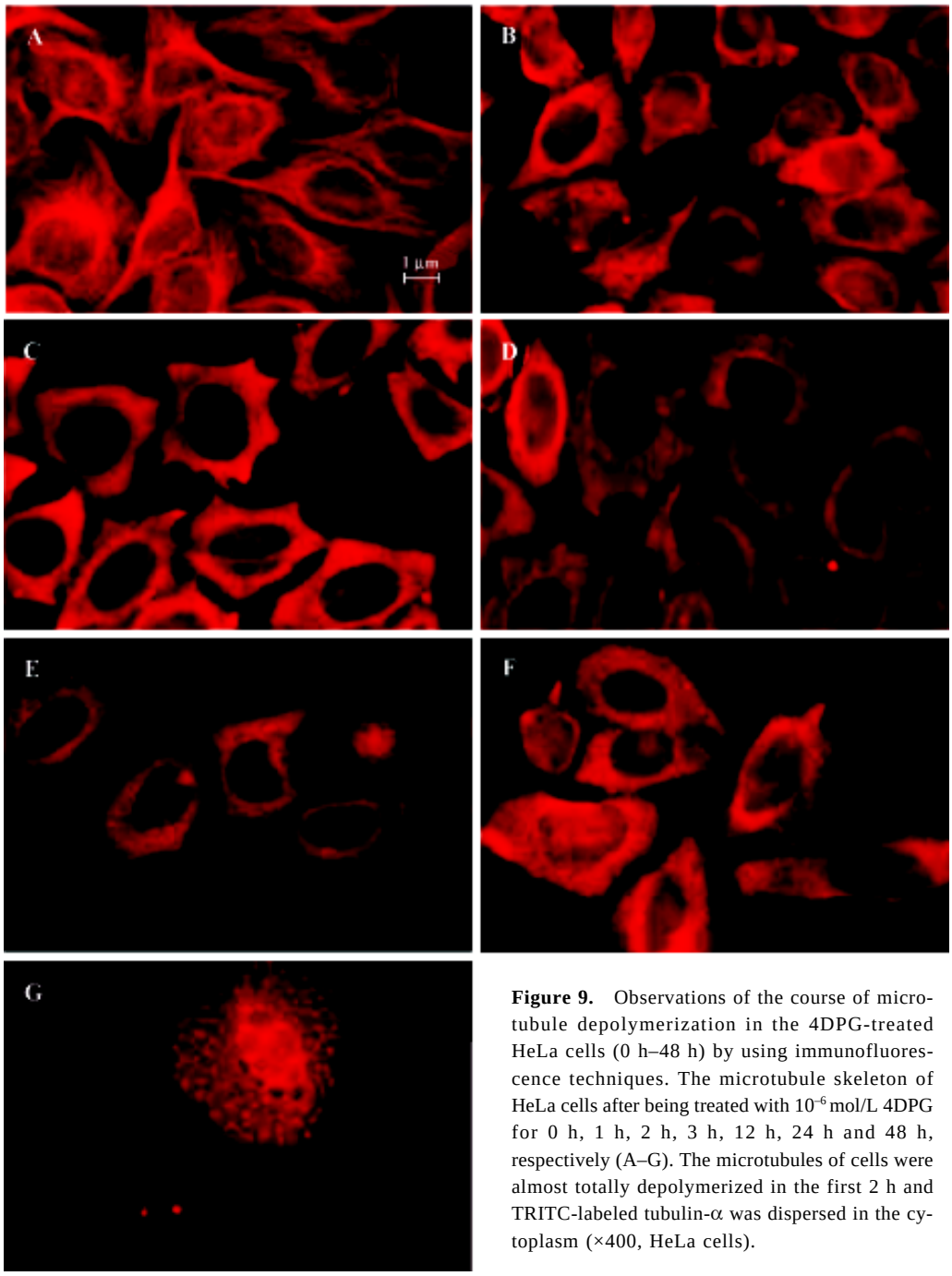

Figure 9. Observations of the course of microtubule depolymerization in the 4DPG-treated HeLa cells (0 h–48 h) by using immunofluorescence techniques. The microtubule skeleton of HeLa cells after being treated with 10^{-6} mol/L 4DPG for 0 h, 1 h, 2 h, 3 h, 12 h, 24 h and 48 h, respectively (A–G). The microtubules of cells were almost totally depolymerized in the first 2 h and TRITC-labeled tubulin-α was dispersed in the cytoplasm (×400, HeLa cells).

as inhibitors of IGF-1R suggest that there is another possible mechanism by which podophyllotoxin inhibits malignant cell proliferation at the same time as it interferes with microtubule assembly[28]. It could be necessary to carry out a study to determine whether 4DPG also possesses this activity.

Microtubules are important cytoskeletal components involved in the regulation of cell proliferation, differentiation, and apoptosis[32]. Microtubule-targeted agents, in particular taxanes[33], have been shown clinically to exert a high level of anticancer activity, and they have also been shown to be promoters of apoptosis in cancer cells[34]. In the present study, the apoptosis-inducing effects of 4DPG were also proven by several observations, including ultrastructure changes, DNA strand breaking and fragmentation, and a subdiploid peak. Apoptosis induced by antimicrotubule

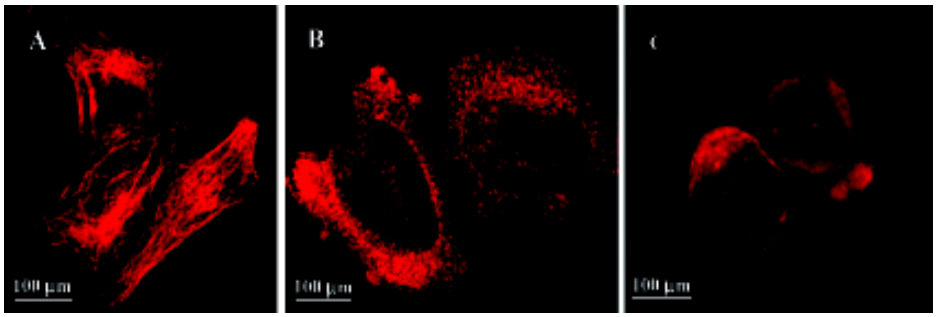

Figure 10. Comparison of the changes in the microtubules of HeLa cells in the control and the 4DPG-treated groups by using confocal immunofluorescence microscopy. (A) The microtubules of normal cells were fibroid and interweaved. (B) When treated with 1×10^{-6} mol/L 4DPG for 24 h, the microtubules of the adherent cells were depolymerized. (C) When treated with 1×10^{-6} mol/L 4DPG for 24 h, most of the suspension cells also disappeared(HeLa cells).

agents is a very complex progress. Many proteins involved in these signal pathways have yet to be identified, and many questions about the process remain unanswered[35,36–38]. It is conceivable that different microtubule binding sites and different disruptions caused by antimicrotubule agents trigger different protein kinase signal pathways. The present study demonstrated clearly that activated caspase-3 increased greatly after treatment with 4DPG for 24 h. This result is quite consistent with the observations gained from TUNEL, suggesting that 4DPG causes the induction of apoptosis through a caspase-3-dependent signaling pathway. The other proteins involved in this apoptotic signaling pathway also need to be determined.

In summary, our results demonstrate that 4DPG has a powerful cytotoxic activity at very low concentrations (<0.01 μmol/L), through interrupting microtubule assembly. It is worth noting that 4DPG is a natural podophyllotoxin glucoside with a unique structure. These findings about the biological activity and mechanism of 4DPG are not only valuable additions to the body of information regarding the structure-activity relationships in the podophyllotoxin family, but also suggest a way forward for exploring natural antitumor products.

References

1 Mukherjee AK, Basu S, Sarkar N, Ghosh AC. Advances in cancer therapy with plant based natural products. Curr Med Chem 2001; 8: 1467–86.
2 Tsai TH. Analytical approaches for traditional Chinese medicines exhibiting antineoplastic activity. J Chromatogr B Biomed Sci Appl 2001; 764: 27–48.
3 Lee KH. Novel antitumor agents from higher plants. Med Res Rev 1999; 19: 569–96.
4 Imbert F. Discovery of podophyllotoxins. Biochimie 1998; 80: 207–22.
5 Cortese F, Bhattacharyya B, Wolf J. Podophyllotoxin as a probe for the colchicine binding site of tubulin. J Biol Chem 1977; 252: 1134–40.
6 Sackett DL. Podophyllotoxin, steganacin and combretastatin: natural products that bind at the colchicine site of tubulin. Pharmacol Ther 1993; 59: 163–228.
7 ter Haar E, Rosenkranz HS, Hamel E, Day BW. Computational and molecular modeling evaluation of the structural basis for tubulin polymerization inhibition by colchicine site agents. Bioorg Med Chem 1996; 4: 1659–71.
8 Desbene S, Giorgi-Renault S. Drugs that inhibit tubulin polymerization: the particular case of podophyllotoxin and analogues. Curr Med Chem Anti-Canc Agents 2002; 2: 71–90.
9 Gordaliza M, Castro MA, del Corral JM, Feliciano AS. Antitumor properties of podophyllotoxin and related compounds. Curr Pharm Des 2000; 6: 1811–39.
10 Gordaliza M, Garcia PA, del Corral JM, Castro MA, Gomez-Zurita MA. Podophyllotoxin: distribution, sources, applications and new cytotoxic derivatives. Toxicon 2004; 44: 441–59.
11 Kelleher JK. Correlation of tubulin-binding and antitumor activities of podophyllotoxin analogs. Cancer Treat Rep 1978; 62: 1443–7.
12 Hainsworth JD, Greco FA. Etoposide: twenty years later. Ann Oncol 1995; 6: 325–41.
13 Schacter L. Etoposide phosphate: what, why, where, and how? Semin Oncol 1996; 23 (Suppl 13): 1–7.
14 Evans WK, Eisenhauer E, Hughes P, Maroun JA, Ayoub J, Shepherd FA, *et al*. VP-16 and carboplatin in previously untreated patients with extensive small cell lung cancer: a study of the National Cancer Institute of Canada Clinical Trials Group. Br J Cancer 1988; 58: 464–8.
15 Splinter T, Kok T, Kho S, Lameris H, ten Kate F, Dalesio O, *et al*. A multicenter phase II trial of cisplatin and oral etoposide (VP-16) in inoperable non-small-cell lung cancer. Semin Oncol 1986; 13 (Suppl 3): 97–103.
16 Aisner J, Lee EJ. Etoposide. Current and future status. Cancer 1991; 67 (Suppl 1): 215–9.
17 Hande KR. Etoposide pharmacology. Semin Oncol 1992; 19 (Suppl 13): 3–9.
18 Minocha A, Long BH. Inhibition of the DNA catenation activity of type II topoisomerase by VP16–213 and VM26. Biochem

Biophys Res Commun 1984; 122: 165–70.
19 Tewey KM, Chen GL, Nelson EM, Liu LF. Intercalative antitumor drugs interfere with the breakage-reunion reaction of mammalian DNA topoisomerase II. J Biol Chem 1984; 259: 9182–7.
20 Long BH and Stringfellow DA. Inhibitors of topoisomerase II: structure-activity relationships and mechanism of action of podophyllin congeners. Adv Enzyme Regul 1988; 27: 223–56.
21 Long BH. Mechanisms of action of teniposide (VM-26) and comparison with etoposide (VP-16). Semin Oncol 1992; 19 (Suppl 6): 3–19.
22 Long BH, Musial ST, Brattain MG. Comparison of cytotoxicity and DNA breakage activity of congeners of podophyllotoxin including VP16-213 and VM26: a quantitative structure-activity relationship. Biochemistry 1984; 23: 1188–94.
23 Paulson JC, McClure WO. Microtubules and axoplasmic transport. Inhibition of transport by podophyllotoxin: an interaction with microtubule protein. J Cell Biol 1975; 67: 461–7.
24 Loike JD, Brewer CF, Sternlicht H, Gensler WJ, Horwitz SB. Structure-activity study of the inhibition of microtubule assembly in vitro by podophyllotoxin and its congeners. Cancer Res 1978; 38: 2688–93.
25 Bedows E, Hatfield GM. An investigation of the antiviral activity of *Podophyllum peltatum*. J Nat Prod 1982; 45: 725–9.
26 Davis RE, Schlumpf BE, Klinger PD. Comparative neurotoxicity of tubulin-binding drugs: inhibition of goldfish optic nerve regeneration. Toxicol Appl Pharmacol 1985; 80: 308–15.
27 Roulland E, Magiatis P, Arimondo P, Bertounesque E, Monneret C. Hemi-synthesis and biological activity of new analogues of podophyllotoxin. Bioorg Med Chem 2002; 10: 3463–71.
28 Girnita A, Girnita L, del Prete F, Bartolazzi A, Larsson O, Axelson M. Cyclolignans as inhibitors of the insulin-like growth factor-1 receptor and malignant cell growth. Cancer Res 2004; 64: 236–42.
29 Vasilcanu D, Girnita A, Girnita L, Vasilcanu R, Axelson M, Larsson O. The cyclolignan PPP induces activation loop-specific inhibition of tyrosine phosphorylation of the insulin-like growth factor-1 receptor. Link to the phosphatidyl inositol-3 kinase/Akt apoptotic pathway. Oncogene 2004; 23: 7854–62.
30 Zhao C, Huang J, Hagatsu A, Ogihara Y. Two new podophyllotoxin glucosides from *Sinopodophyllum emodi* (Wall) Ying. Chem Pharm Bull 2001; 49: 773–5.
31 Mosmann T. Rapid colorimetric assay for cellular growth and survival: application to proliferation and cytotoxicity assays. J Immunol Methods 1983; 65: 55–63.
32 Gundersen GG, Cook TA. Microtubules and signal transduction. Curr Opin Cell Biol 1999; 11: 81–94.
33 Miller KD, Sledge GW Jr. Taxanes in the treatment of breast cancer: a prodigy comes of age. Cancer Invest 1999; 17: 121–36.
34 Mollinedo F, Gajate C. Microtubules, microtubule-interfering agents and apoptosis. Apoptosis 2003; 8: 413–50.
35 Jordan MA, Wendell K, Gardiner S, Derry WB, Copp H, Wilson L. Mitotic block induced in HeLa cells by low concentrations of paclitaxel (Taxol) results in abnormal mitotic exit and apoptotic cell death. Cancer Res 1996; 56: 816–25.
36 Tseng CJ, Wang YJ, Liang YC, Jeng JH, Lee WS, Lin JK, *et al*. Microtubule damaging agents induce apoptosis in HL60 cells and G2/M cell cycle arrest in HT29 cells. Toxicology 2002; 175: 123–42.
37 Wang LG, Liu XM, Kreis W, Budman DR. The effect of antimicrotubule agents on signal transduction pathways of apoptosis: a review. Cancer Chemother Pharmacol 1999; 44: 355–61.
38 Bhalla KN. Microtubule-targeted anticancer agents and apoptosis. Oncogene 2003; 22: 9075–86.